Materials Advances

ROYAL SOCIETY OF CHEMISTRY

PAPER

View Article Online
View Journal | View Issue

Cite this: *Mater. Adv.*, 2022, 3, 6000

Effects of a polystyrene intermediate layer for improved electrochromic properties of nano porous WO_3 electrochromic films

Dipti. R. Sahu, *[a] Cheng-Yen Hung,[b] Sheng-Chang Wang[c] and Jow-Lay Huang[bde]

Nanostructured electrochromic materials having long life cycle and high chemical stability are promising for displays, rear view mirrors, and smart window applications. In the present study, nano tungsten trioxide (WO_3) films are prepared using a low-cost conventional spin coating method. The porosity of the WO_3 layers is developed using a polystyrene intermediate layer in order to improve the cyclic stability of the film. The structural characterization using X-ray diffraction confirms the formation of the orthorhombic phase. Surface studies *via* atomic force microscopy and scanning electron microscopy show a porous network along with a change in the roughness of the films. Electrochromic study using a potentiostat, UV-visible spectrophotometer and the voltammetry method indicate that a porous crystalline WO_3 has a stable coloration efficiency, durability, and fast response to the electrochromic cycle with higher transmittance in comparison with nonporous WO_3 films. The crystalline film with a porous structure shows a transmission modulation of about 65.3% and 10% more coloration efficiency than the nonporous film. The electrochromic properties of the crystalline nonporous film deteriorate at/after 500 °C. The porous structure improves the chemical stability of the film with long durability and solves the problem of degradation of the film after long hours of operation for an electrochromic device.

Received 28th April 2022,
Accepted 11th June 2022

DOI: 10.1039/d2ma00476c

rsc.li/materials-advances

1. Introduction

Progress in nanotechnology creates numerous materials with good physical and chemical properties for different applications.[1–3] One of such materials is the nano tungsten oxide (WO_3), which is widely known as an electrochromic (EC) material. Electrochromic WO_3 has application as rearview mirrors, automobile glazing, smart sunglasses, and smart windows.[4–6]

Since the first reported work on the electrochromism of WO_3,[7] this material has been continuously researched for improving its properties, understanding its physics and developing devices using WO_3.[6,8–10] In general, there are interstitial sites in WO_3 where foreign materials or ions can be inserted easily to change the behaviour of the EC material.[11,12] It is known that in its fully occupied state WO_3 is transparent but it reaches the EC state after electrochemical reduction.[13]

Currently, the anodic oxidation method is normally used for the manufacture of WO_3 thin films.[14,15] Porosity, thickness, crystallinity, composition, and stoichiometry are important factors that influence the electrochromic properties of WO_3 thin filmw.[16–19] Our previous study on a WO_3 film synthesized by a chemical method shows that the film exhibited optimum electrochromic properties in its crystalline phase; however, the chemical stability and coloration efficiency of the film deteriorates after a long cycle of operation.[20] Therefore, there is a need to improve the electrochromic behaviour of the film by maintaining the stability of the electrochromic properties during applications. It is reported that a high film porosity will enhance the surface area and improve the electrochromic properties of films.[21,22] The growth of a porous electrochromic film can increase the color/bleach rate, extend durability, stabilize electrochromic properties, and increase its lifetime.[1,6,12] The production of environment friendly WO_3 can advance the research in the electrochromic film fabrication and its application in glass window films. The goal of this study is to improve the chemical stability of the film by prolonging the cyclic durability and improving the electrochromic properties without degradation

[a] *Department of Natural and Applied Sciences, Namibia University of Science and Technology, Private Bag 13388, Windhoek, Namibia. E-mail: dsahu@nust.na; Fax: +264-6-2079783; Tel: +264-6-2072783*
[b] *Department of Materials Science and Engineering, National Cheng-Kung University, Tainan, 701, Taiwan*
[c] *Department of Mechanical Engineering, Southern Taiwan University of Science and Technology, Tainan, 710, Taiwan*
[d] *Center for Micro/Nano Science and Technology, National Cheng Kung University, Tainan, 701, Taiwan*
[e] *Hierarchical Green-Energy Materials (Hi-GEM) Research Center, National Cheng Kung University, Tainan, 701, Taiwan*

for device application. Therefore, in this study, nano porous WO_3 films are prepared with a solgel processed precursor solution using a low-cost conventional spin coating method. The porosity of the WO_3 layers is generated using the polystyrene as an intermediate layer. The porous crystalline WO_3 film shows a stable coloration efficiency of 24 cm^2 C^{-1}, transmittance modulation effect of 65.3% and good electrochromic properties up to 1000th cycle of operation, which is much better than other reported literature data.[20–23] In literature, only few doped films show good coloration efficiency but they degrade after long cycle of operations, while other few films are not stable without doping that changes the electrochromic properties after a cycle of operation.[22,23] Herein, the observed electrochromic properties are much better in the prepared pure porous crystalline WO_3 film in terms of coloration efficiency and transmission modulation compared with nonporous WO_3 films.

2. Experimental details

Nano porous WO_3 films were prepared using spin coating and solgel method. The precursor solution was synthesized by the sol-gel method. WCl_6 was dissolved in isopropanol and acetic acid. Acetic acid played the role of a chelating agent for the preparation of the precursor. The precursor solution was stirred fully for 30 min and then 2 ml of H_2O_2 was added into the precursor to act as a strong oxidizing agent. Then, the spin coating of WO_3 was done on an indium tin oxide (ITO) substrate. The ITO substrate was ultrasonically cleaned in acetone, isopropanol and deionized water, respectively, and then dried by blowing nitrogen. First, one WO_3 layer was prepared by spin coating on an ITO substrate at 300 rpm. Then, the films were heat-treated at 100 °C to remove the solvent. Then, the polystyrene latex microsphere (0.2 micron) dispersed in 2.5 wt% water was deposited on the WO_3 layer, which acted as an intermediate layer in order to generate the porosity of the WO_3 film. Furthermore, a second layer of WO_3 was deposited above the polystyrene layer using spin coating at 3000 rpm. The deposited film on the ITO with polystyrene was heated at a temperature of 200 °C to remove the polystyrene and make the film porous. As per our previous study in this case, the thickness of the porous film was also kept at about 150 nm. Further heat treatment was performed at a rate of 5 °C min^{-1} at 250 and 500 °C for 2 h for the phase formation of WO_3. The details about the phase formation, preparation and deposition of WO_3 films using the spin coating method were mentioned elsewhere.[20]

The structural properties of the prepared films were studied by a D/Max-II X-ray diffractometer (XRD) with CuKα radiation. The surface morphology the films was studied using a XL 40 Philips scanning electron microscope (SEM) at an operative voltage of 10 kV. The accelerating voltage of the SEM was in the range of 5–30 kV. Atomic force microscopy (AFM) images were acquired using a Digital Instrument INC, NanoScope, California, USA. The electrochromic properties of the films were studied by cyclic voltammetry. The cyclic voltammogram test was carried out on a Versastat II electrochemical workstation of a three-electrode cell system with an electrolyte solution of 0.5 M lithium perchlorate in propylene carbonate ($LiClO_4$/PC). The working electrode was made of tungsten oxide film on the ITO substrate. The reference and counter electrodes were a saturated calomel electrode (SCE) and a platinum grid, respectively. The transmittance spectra of the films were recorded in the 300–800 nm wavelength range using the Hitachi U-2001 UV-visible spectrophotometer.

3. Results and discussion

It is known from our previous study[20] and reported literature[23–25] that the crystal structure of WO_3 is generally dependent on the growth of the film on different substrates using different methods and annealing temperatures. The as-deposited film annealed at 300 °C is amorphous and the film annealed at 500 °C is crystalline. Similar to previous studies and this study, the XRD data of nonporous and porous crystalline films match well with the JCPDS PDF 20-1324 data.[26]

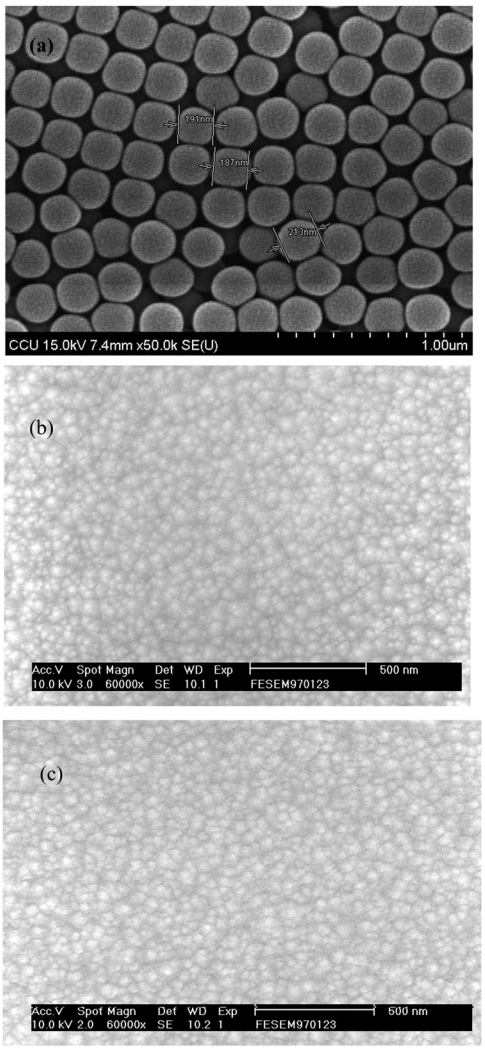

Fig. 1 SEM micrograph of the WO_3 film (a) polystyrene latex microsphere (b) annealed porous film (c) porous crystalline film.

The XRD results indicate that the film structure is orthorhombic in nature.

Fig. 1 presents the SEM micrograph of the WO_3 film. The surface morphology of the film shown in Fig. 1(a) indicates that the polystyrene latex microsphere dispersed in 2.5 wt% water is well deposited on the surface of the WO_3 layer. The polystyrene latex microsphere ranges between 185 nm and 215 nm in size. The film with a single layer of WO_3 deposited with the polystyrene sphere looks smooth and well arranged. Fig. 1(b) presents the porous structure on the annealed film at 300 °C where another layer of WO_3 is deposited on the polystyrene sphere. The WO_3 film looks porous with a nanoscale interconnecting network, which is similar to the reported literature.[27] The WO_3 film looks like a random porous island structure. Fig. 1(c) shows the micrograph of the crystalline WO_3 film annealed at 500 °C. The morphologies of the WO_3 film show changes in the structure. The WO_3 pore sizes increase with the annealing and change the film behaviour as the film becomes fully crystalline. The porous WO_3 film may have more open space among the materials, which allows the polystyrene sphere to penetrate through the film and make the film well defined by the crystalline structure. This nanoporous morphology and structure with the intragranular contact effectively improve the electrochromic behaviour of the film, which can be controlled by the polystyrene sphere and annealing temperature.[28,29]

Fig. 2(a and b) shows the atomic force micrograph of the crystalline and porous crystalline WO_3 films, respectively. The images show a roughness value of about 2.08 nm (Fig. 2(a)) for the nonporous crystalline film, which increases to 69.02 nm (Fig. 2(b)) for the porous crystalline film. However, the roughness of the as deposited film is 13.92 nm (images not shown here) that decreases to 2.08 nm by annealing at 500 °C temperature. This indicates that the polystyrene sphere, which is porous in structure, can change the roughness of the film with annealing. The annealed porous crystalline films are much rougher than the as-deposited amorphous films.[30]

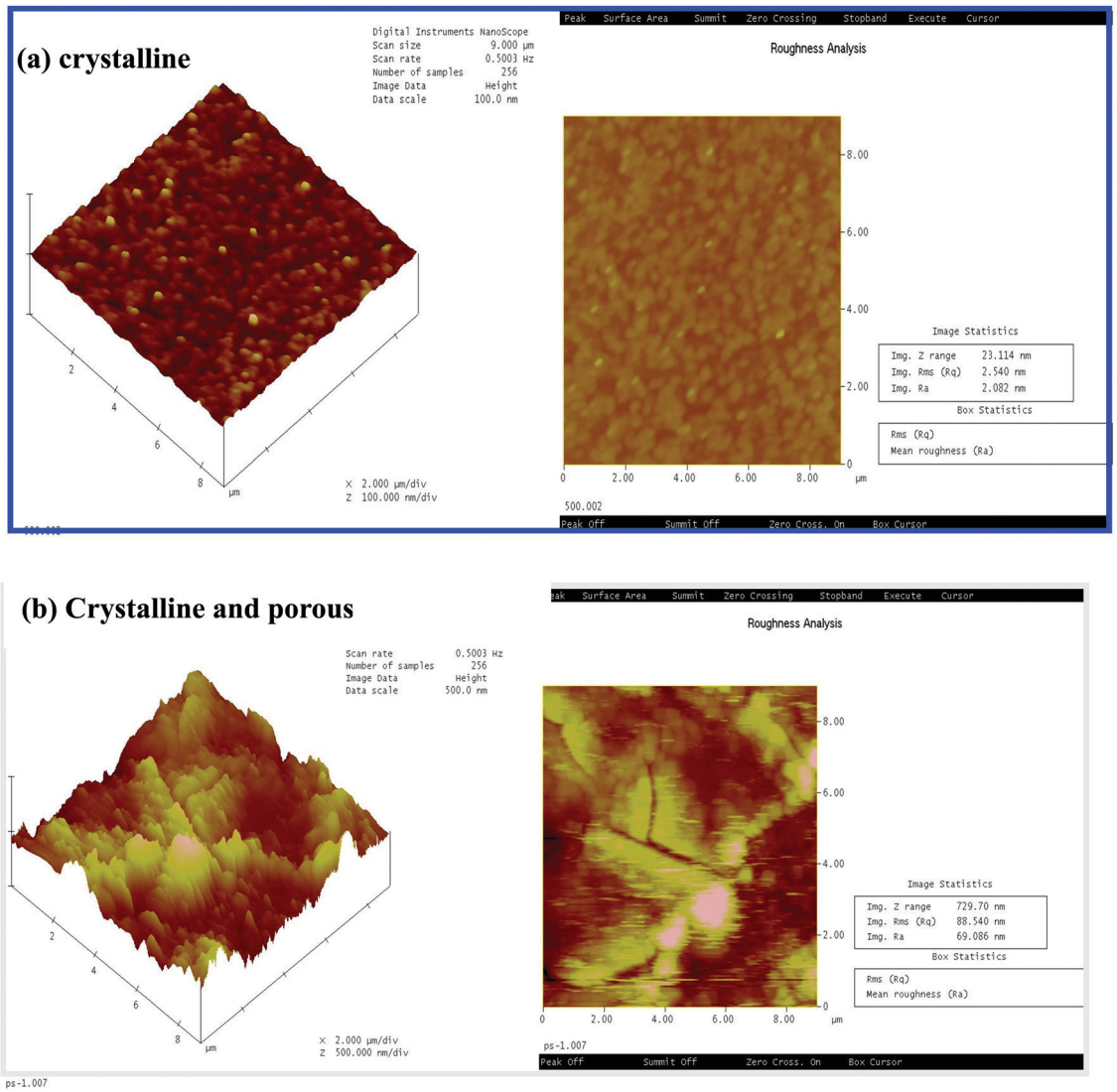

Fig. 2 AFM images of the as-deposited and annealed (a) crystalline and (b) porous crystalline WO_3 films.

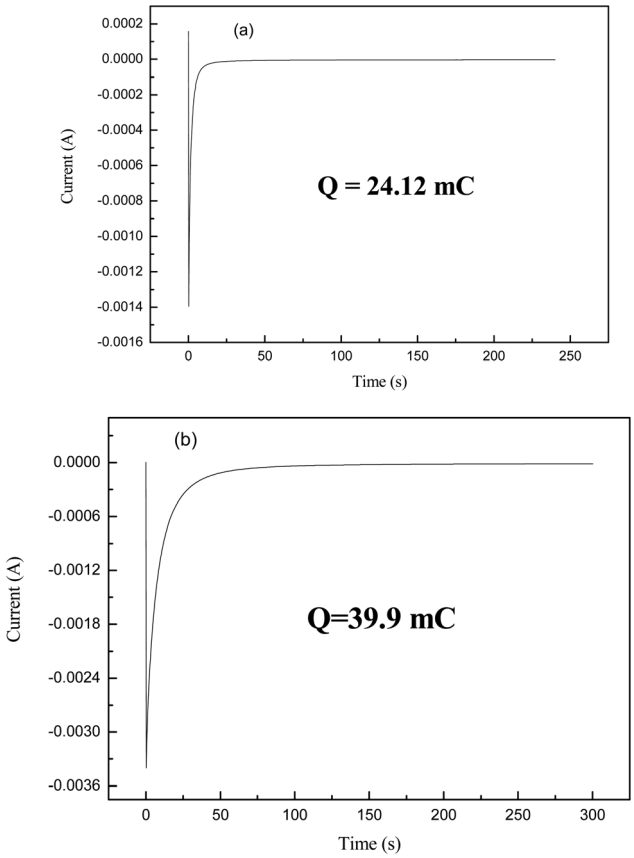

Fig. 3 Potential step spectrum of WO_3 films (a) nonporous (b) porous crystalline.

The potential step spectrum of the WO_3 films present in Fig. 3 for the nonporous and porous crystalline states indicates that the porous crystalline WO_3 films have an insertion ability of about 39.9 mC, which is higher than the nonporous crystalline film. This indicates that when the film becomes porous, an increase in the surface area is observed, and thus, the ion insertion capability increases apparently, which enhances the electrochromic behaviour of the film.[31]

Fig. 4 presents the transmittance spectra of nonporous and porous crystalline WO_3 films. The transmittance spectra for the nonporous film are more porous than the crystalline film in colored state. There is no significant difference between the transmittance spectra. However, the trend of transmittance spectra is different for both films. For the nonporous crystalline film, the transmittance is increasing in the visible region and then it decreases in the long wavelength region. On the contrary, the porous crystalline film trend initially decreases in the visible region, and then it increases continuously in the long wavelength region up to 1100 nm. The maximal transmittance of the porous film increases to 25% while the nonporous film is reduced to 10%. In the visible region, the maximum transmittance of about 60% is achievable for the crystalline nonporous film. However, in the bleached state, both films show higher transmittances. The porous crystalline WO_3 film exhibits a transmittance modulation effect of 65.3%. However the nonporous

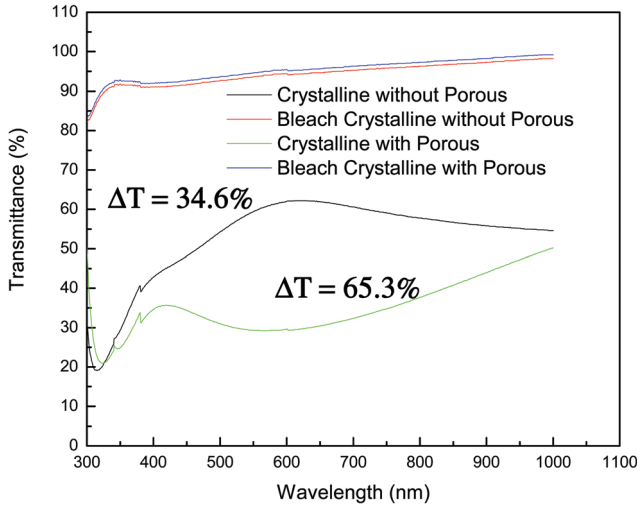

Fig. 4 The transmittance spectra of nonporous and porous crystalline WO_3 films in coloured and bleached states.

Table 1 Electrochromic properties of WO_3 films

	Crystalline without porous	Crystalline with porous
ΔT (%)	34.6	65.3
Q_{in} (mC)	24.12	39.9
CE (cm^2 C^{-1})	14.12	24

film shows a modulation of 34.6%. The nonporous film shows more than 30% modulation in the colored and bleached states. Due to the increase in the surface area in the porous film, more charge intercalation occurs, which affects the transmittance of the films. The detailed electrochromic results are listed in Table 1.

Fig. 5 shows the electrochromic cyclic voltammogram (CV) curves for the porous crystalline films at different cycles of operation. The CV curves indicate that there is a change in the peak positions with the incorporation of an injected charge.[32]

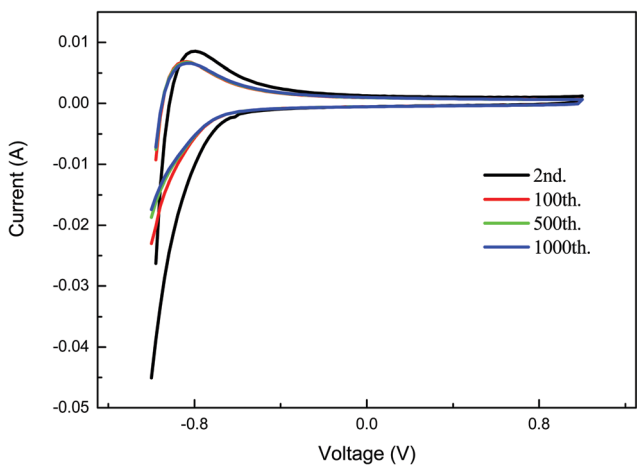

Fig. 5 The electrochromic cyclic voltammogram (CV) curves for the porous crystalline films for different cycles of operation.

The film shows good electrochromic behaviour up to the 1000th cycle of operation and there is a decrease in the integral area during the operation cycle. This indicates that the electrochemical reaction is occurring in the film during the cycle of operation. The films show stable electrochromic properties. The porous crystalline film is not degraded after the operation.

The durability of the films after the electrochromic cycle is studied in terms of charge intercalation, and the results are shown in Fig. 6. It is observed that there is a variation in charge intercalation for each film after the cycle of operation. The charge intercalation increases for the crystalline film, almost remains constant for the porous crystalline film, and decreases rapidly for the amorphous films. The effect of grain boundary and reaction generally changes the relative capacity of charge intercalation in the film. The porous crystalline film shows a good crystalline structure and uniform grain size; therefore, it maintains almost the same amount of charge intercalation after a long cycle of operation. The film structure, morphology and electrolytes affect the intercalation/deintercalation processes.[33,34] This charge intercalation also affects the transmittance modulation and cyclic life of the film.[35] In this study, the porous film shows stable and improved electrochromic properties as porous crystalline film aggregation does not take place and the film did not reach its steady state.

The coloration efficiency (CE) defined as $CE = \Delta OD/Q_{in}$,[36] where ΔOD is the change in the optical density with charges intercalated per unit electrode area and Q_{in} is the charge intercalated per unit area, is used to study the intrinsic material property. Herein, $\Delta OD = \log (T_{bleaching}/T_{coloring})$ where $T_{bleaching}$ is the transmittance in the bleached state and $T_{coloring}$ is the transmittance in the colored state. The CE analysis shows that the porous crystalline film has 24 $cm^2\ C^{-1}$ efficiency while the crystalline film has 14 $cm^2\ C^{-1}$. The CE is almost constant up to the 1000th cycle for the porous crystalline film mainly due to the constant amount of charge intercalation during the long cycle of operation.[37,38] This indicates that the grown film has good durability. However, the CE is not constant for the amorphous film during the cycle of operation. This may be due to the change in the charge intercalation during the cycle of operation.[39,40] As there is no change in the CE value after the long cycle of operation, it indicates that the films are of good quality with stable morphology after the electrochromic cycle.[41–43] In our earlier study,[20] it was found that the electrochromic coloration behaviours of the amorphous and crystalline films are not stable, the transmission modulation decreases, and films degrade after long cycles of operation. However, this porous crystalline film shows stable coloration efficiency, durability, and fast response to the electrochromic cycle with higher transmittance, which are prerequisites for smart window applications. The growth of the porous electrochromic film can solve the problem of the degradation of the film after long hours of operation in a device.

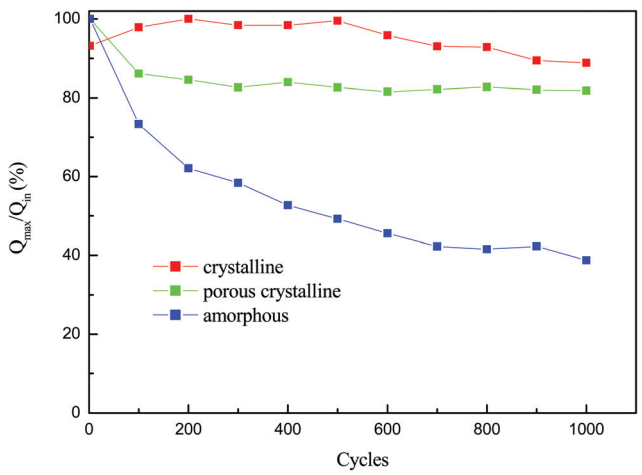

Fig. 6 Q_{in}/Q_{max} *vs.* cycle's spectrum of WO_3 films at amorphous, porous crystalline and crystalline states.

4. Conclusions

Good quality nano WO_3 films were fabricated successfully with improved stable electrochromic properties up to 1000 cycles of operation. The porous structure improves the chemical stability and durability of the films. The growth of porous crystalline films using the spin coating method has a unique advantage of overcoming the degradation problem with remarkable electrochromic properties. The film shows stable coloration efficiency of about 24 $cm^2\ C^{-1}$, greater transmittance modulation and durability which are perfect for processing effective electrochromic films for device applications.

Conflicts of interest

There are no conflicts to declare.

Acknowledgements

The financial support received for Hierarchical Green-Energy Materials (Hi-GEM) Research Center, Tainan and RPRC, Namibia University of Science and Technology, Windhoek, Namibia for this work is highly acknowledged.

References

1 Y. Djaoued, S. Balaji and R. Brüning, Electrochromic devices based on porous tungsten oxide thin films, *J. Nanomater.*, 2012, **9**, 674168.
2 S. Bulja, R. Kopf, A. Tate, T. Hu, R. Cahill, M. Norooziarab, D. Kozlov, P. Rulikowski and W. Templ, Electro-chromic structure with a high degree of dielectric tunability, *Sci. Rep.*, 2019, **9**, 107731.
3 J. Mohelniova, Materials for reflective coatings of window glass applications, *Constr. Build. Mater.*, 2009, **23**(5), 1993–1998.
4 W. Zhang, H. Li, E. Hopmann and A. Y. Elezzabi, Nanostructured inorganic electrochromic materials for light applications, *Nanophotonics*, 2020, **10**(2), 825–850.

5 N. N. Dinh, D. H. Ninh, T. T. Lao and T. V. Van, Mixed nanostructured Ti-W oxides films for efficient electrochromic windows, *J. Nanomater.*, 2012, **7**, 781236.
6 Qingfei Wu, Jing Huang and Hua Li, Deposition of porous nano-WO_3 coatings with tunable grain shapes by liquid plasma spraying for gas-sensing applications, *Mater. Lett.*, 2015, **141**, 100–103.
7 H. Byker, in *Electrochromic Materials II, PV 94-2, Electrochemical Society Proceeding Series*, ed. K. C. Ho and D. A. MacArthur, Pennington, NJ, 1994, pp. 3–13.
8 C. G. Granqvist, M. A. Arvizu, I. B. Pehlivan, H. Y. Qu, R. T. Wen and G. A. Niklasson, Electrochromic materials and devices for energy efficiency and human comfort in buildings: a critical review, *Electrochim. Acta*, 2018, **259**, 1170–1182.
9 S. Jin Lee, T.-G. Lee, S. Nahm, D. H. Kim, D. J. Yang and S. H. Han, Investigation of all-solid-state electrochromic devices with durability enhanced tungsten-doped nickel oxide as a counter electrode, *J. Alloys Compd.*, 2020, **815**, 152399, DOI: 10.1016/j.jallcom.2019.152399.
10 R. J. Mortimer, A. L. Dyer and J. R. Reynolds, Electrochromic organic and polymeric materials for display applications, *Displays*, 2006, **27**, 2–18.
11 V. R. Buch, A. K. Chawla and S. K. Rawal, Review on electrochromic property for WO_3 thin films using different deposition technique, *Mater. Today: Proc.*, 2016, **3**(6), 1429–1437.
12 C. C. Chen, Characterization of Porous WO_3 Electrochromic Device by Electrochemical Impedance Spectroscopy, *J. Nanomater.*, 2012, **14**, 785023.
13 P. R. Somani and S. Radhakrishnan, Electrochromic materials and devices: present and future, *Mater. Chem. Phys.*, 2003, **77**(1), 117–133.
14 C. Cai, D. Guan and Y. Wang, Solution processing of V_2O_5-WO_3 composite films for enhanced Li-ion intercalation properties, *J. Alloys Compd.*, 2010, **509**(3), 909–915.
15 V. Karastoyanov and M. Bojinov, Anodic oxidation of tungsten in sulphuric acid solution-Influence of hydrofluoric acid addition, *Mater. Chem. Phys.*, 2008, **112**(2), 702–710.
16 S. Supothina, P. Seeharaj, S. Yoriya and M. Sriyudthsak, Synthesis of tungsten oxide nanoparticles by acid precipitation method, *Ceram. Int.*, 2007, **33**(6), 931–936.
17 M. Gratzel, Ultrafast colour displays, *Nature*, 2001, **409**, 575–576.
18 C. G. Granqvist, Electrochromics for smart windows: Oxide-based thin films and devices, *Thin Solid Films*, 2014, **564**, 1–38.
19 G. F. Cai, X. Wang, M. Q. Cui, P. Darmawan, J. X. Wang, A. L.-S. Eh and P. S. Lee, Electrochromo-supercapacitor based on direct growth of NiO nanoparticles, *Nano Energy*, 2015, **12**, 258–267.
20 D. R. Sahu, C. Y. Hung and S. C. Wang, Jow-Lay Huang, Existence of electrochromic reversibility at the 1000th cyclic voltammetry for spin coating WO_3 film, *Ionics*, 2017, **23**, 3227–3233.
21 W. J. Lee, Y. K. Fang, J.-J. Ho and F. C. Ho, Effects of surface porosity on tungsten trioxide(WO_3) films' electrochromic performance, *J. Electron. Mater.*, 2018, **29**(2), 183–187.
22 Y. Yang, Y. Qi, W. Zhai, J. Tan, S. Feng, J. Zhang, M. Shen, L. Wang, X. Yu and X. Qu, Enhanced Electrochromic Performance of Film Based on Preyssler-Type Polyoxometalate and Tungsten Oxide, *Electron. Mater. Lett.*, 2020, **16**, 424–432.
23 K. P. R. Rao, V. C. Babu, V. R. Kumar and N. Veeriah, Characterization and coloration efficiency studies using cyclicvoltammetry and chronocoulometric methods on TiO_2 doped WO_3 nanocrystalline thin films, *Optik*, 2022, **249**, 168282.
24 C. V. Ramana, S. Utsunomiya, R. C. Ewing, C. M. Julien and U. Becker, Structural Stability and Phase Transitions in WO_3 Thin Films, *J. Phys. Chem. B*, 2006, **110**, 10430.
25 T. Vogt, P. M. Woodward and B. A. Hunter, The high-temperature phases of WO_3, *J. Solid State Chem.*, 1999, **144**, 209.
26 Y. C. Liang and C. W. Chang, Preparation of Orthorhombic WO3 Thin Films and Their Crystal Quality-Dependent Dye Photodegradation Ability, *Coatings*, 2019, **9**, 1–11, DOI: 10.3390/coatings9020090.
27 G. Cai, M. Cui, V. Kumar, P. Darmawan, J. Wang, X. Wang, A. L.-S. Eh, K. Qian and P. S. Lee, Ultra-large optical modulation of electrochromic porous WO_3 film and the local monitoring of redox activity, *Chem. Sci.*, 2016, **7**, 13.
28 S. Badilescu and P. V. Ashrit, Study of sol–gel prepared nanostructured WO_3 thin films and composites for electrochromic applications, *Solid State Ionics*, 2003, **158**(1–2), 187–197.
29 M. Deepa, A. G. Joshi, A. K. Srivastava, S. M. Shivaprasad and S. A. Agnihotry, Electrochromic Nanostructured Tungsten Oxide Films by Sol-gel: Structure and Intercalation Properties, *J. Electrochem. Soc.*, 2006, **153**, C365.
30 A. A. Joraid, Comparison of electrochromic amorphous and crystalline electron beam deposited WO3 thin films, *Curr. Appl. Phys.*, 2009, **9**, 73.
31 C. Cai, D. Guan and Y. Wang, Solution processing of V_2O_5–WO_3 composite films for enhanced Li-ion intercalation properties, *J. Alloys Compd.*, 2011, **509**, 909–915.
32 M. Guziewicz, J. Grochowski, M. Borysiewicz, E. Kaminska, J. Z. Domagala, W. Rzodkiewicz, B. S. Witkowski, K. Golaszewska, R. Kruszka, M. Ekielski and A. Piotrowska, Electrical and optical properties of NiO films deposited by magnetron sputtering, *Opt. Appl.*, 2011, **XLI**(2), 431–440.
33 D. S. Dalavi, M. J. Suryavanshi, D. S. Patil, S. S. Mali, A. V. Moholkar, S. S. Kalagi, S. A. Vanalkar, S. R. Kang, J. H. Kim and P. S. Patil, Nanoporous nickel oxide thin films and its improved electrochromic performance: effect of thickness, *Appl. Surf. Sci.*, 2011, **257**, 2647–2656.
34 A. Azens, L. Kullman, G. Vaivars, H. Nordborg and C. G. Granqvist, Sputter-deposited nickel oxide for electrochromic applications, *Solid State Ionics*, 1998, **113e115**, 449–456.
35 I. Bouessay, A. Rougier and J. M. Tarascon, Electrochemically inactive nickel oxide as electrochromic material, *J. Electrochem. Soc.*, 2004, **151**, H145–H152.
36 S. Pereira, A. Goncalves, N. Correia, J. Pinto, L. Pereira, R. Martins and E. Fortunato, Electrochromic behaviour

of NiO thin films deposited by e-beam evaporation at room temperature, *Sol. Energy Mater. Sol. Cells*, 2014, **120**, 109–115.

37 A. Edgar, Rojas-Gonzáleza) and Gunnar A. Niklasson, Differential coloration efficiency of electrochromic amorphous tungsten oxide as a function of intercalation level: Comparison between theory and experiment, *J. Appl. Phys.*, 2020, **127**, 205101.

38 M. Fabretto, T. Vaithianathan, C. Hall, P. Murphy, P. C. Innis, J. Mazurkiewicz and G. G. Wallace, Colouration efficiency measurements in electrochromic polymers: The importance of charge density, *Electrochem. Commun.*, 2007, **9**, 2032–2036.

39 J. Nagai, G. D. McMeeking and Y. Saitoh, Durability of electrochromic glazing, *Sol. Energy Mater. Sol. Cells*, 1999, **56**(3-4), 309–319.

40 D. Mansoura, O. Bouvarda and A. Schülera, Development and characterization electrochromic oxide and ion conductor deposited by reactive magnetron sputtering, *Energy Procedia*, 2017, **122**, 787–792.

41 Z. Xie, Q. Liu, Q. Zhang, B. Lu, J. Zha and X. Diao, Fast-switching quasi-solid state electrochromic full device based on mesoporous WO_3 and NiO thin films, *Sol. Energy Mater. Sol. Cells*, 2019, **200**, 110017.

42 R.-T. Wen, G. A. Niklasson and C. G. Granqvist, Sustainable rejuvenation of electrochromicWO3 films, *ACS Appl. Mater. Interfaces*, 2015, 7(51), 28100–28104.

43 D. Dong, W. Wang, A. Rougier, G. Dong, M. Da Rocha, L. Presmanes, K. Zrikem, G. Song, X. Diao and A. Barnab, Life-cycling and uncovering cation-trapping evidence of a monolithic inorganic electrochromic device: glass/ITO/WO3/LiTaO3/NiO/ITO, *Nanoscale*, 2018, **10**(35), 16521–16530.